

Deutscher Wetterdienst
Wetter und Klima aus einer Hand



RAL Space



SMHI



Royal Netherlands
Meteorological Institute
Ministry of Transport, Public Works
and Water Management



ETH

ESA Cloud_cci

Report on orbital drift correction for AVHRR




Issue 1 Revision 1

28 August 2017

Deliverable No.:	D2.1
ESRIN/Contract No.:	4000109870/13/I-NB
Project Coordinator:	Dr. Rainer Hollmann Deutscher Wetterdienst rainer.hollmann@dwd.de
Technical Officer:	Dr. Simon Pinnock European Space Agency Simon.Pinnock@esa.int



	Doc:	Cloud_cci_D2.1_ATBD-RODC_v1.1.doc			
	Date:	28 August 2017			
	Issue:	1	Revision:	1	Page 2

Document Change Record

Document, Version	Date	Changes	Originator
V1.0	11/05/2017	First issued version	Abhay Devasthale, Karl-Göran Karlsson, Martin Stengel Rainer Hollmann
V1.1	28/08/2017	Revision after ESA review	Abhay Devasthale, Martin Stengel

Purpose

The purpose of this document is to assess methods for correcting the impact of the orbital drift of NOAA's AVHRR-carrying polar-orbiting satellites on AVHRR-based cloud climatologies generated in Cloud_cci.



	Doc:		Cloud_cci_D2.1_ATBD-RODC_v1.1.doc		
	Date:		28 August 2017		
	Issue:	1	Revision:	1	Page 3

Table of Contents

1. Introduction	4
2. Impact of orbital drift on clouds.....	6
3. Possible approaches to account for orbital drift effect	7
4. Application of diurnal cycle based methodology to ESA Cloud_cci AVHRR-AM/PM datasets	8
5. Evaluating diurnal cycles and some problem areas	14
6. Applying REOFs to correct orbital drift effect	18
7. Summary	21
8. References	22
9. Glossary	24

	Doc:	Cloud_cci_D2.1_ATBD-RODC_v1.1.doc		
	Date:	28 August 2017		
	Issue:	1	Revision:	1
Page 4				

1. Introduction

The ESA Cloud_cci project pursues the development of coherent long-term cloud property datasets (Hollmann et al., 2013, Stengel et al., 2015). These product-based climate datasets (formally denoted Thematic Climate Data Records - TCDRs) were derived from accurately calibrated and homogenized radiances (formally denoted Fundamental Climate Data Records - FCDRs). The FCDRs build the basis for the Essential Climate Variable (ECV) datasets. These ECV datasets were derived using the two physical retrieval systems Community Cloud retrieval for Climate (CC4CL; Sus et al., 2017; McGarragh et al., 2017) and Freie Universität Berlin AATSR MERIS Cloud retrieval (FAME-C; Carbajal Henken et al., 2014). CC4CL is an open community code, with algorithm developments taken place during the ongoing project. After applying the retrieval systems for the generation of the Cloud_cci datasets, the validation of cloud products, the provision of a common data base and the feasibility of accessing the cloud data were implemented and have been maintained. The final processing system as described in this document builds a sound basis for any future reprocessing of CC4CL and FAME-C based datasets and a potential operational production of cloud data also beyond the expiration of the Cloud_cci project.

The objective of Cloud_cci has been the generation of two product families. The first family is an (A)ATSR/SLSTR-MODIS-AVHRR heritage product group. Products for this family were derived using CC4CL applied to instrument channels matching those available from the AVHRR “heritage” channel set. In this family, cloud properties are separately derived from AATSR/SLSTR (and the ATSR-series), MODIS and AVHRR. The second product family includes cloud properties derived using FAME-C applied to combined AATSR and MERIS measurements set using a synergistic retrieval approach. CC4CL and FAME-C are also able to process successor system data of SLSTR/OLCI on board the Sentinel-3 satellite. Considering the spectral, imaging and observational characteristics of the considered sensors, the following Cloud_cci datasets were defined:

- AVHRR-AM (S: NOAA-12, NOAA-15, NOAA-17, Metop-A; A: CC4CL, PC: DWD)
- AVHRR-PM (S: NOAA7, NOAA9, NOAA11, NOAA14, NOAA16, NOAA18, NOAA19; A: CC4CL; PC: DWD)
- MODIS-Terra (S: Terra; A: CC4CL; PC: DWD)
- MODIS-Aqua (S: Aqua; A: CC4CL; PC: DWD)
- ATSR2-AATSR (S: ERS-2, Envisat; A: CC4CL; PC: RAL)
- MERIS-AATSR (S: Envisat; A: FAME-C; PC: FUB)

where S indicates the satellites covered, A the algorithm used and PC the processing center. Figure 1-1 shows the datasets and the time periods they cover.

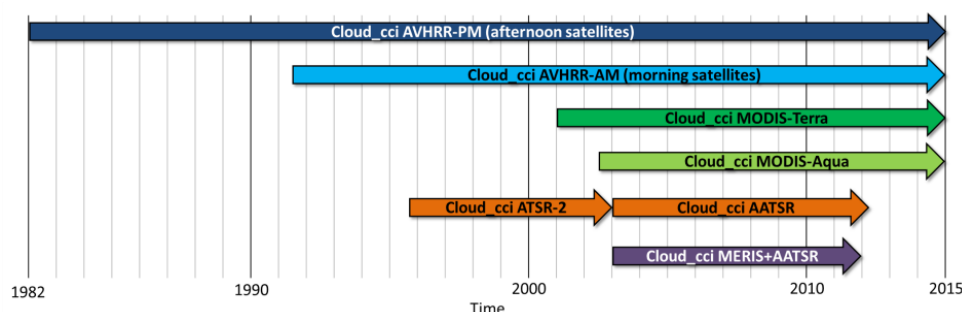



Figure 1-1 Overview of Cloud_cci datasets and the time periods they cover.

The Cloud_cci AVHRR-AM and AVHRR-PM datasets are based on AVHRR measurements available as Global Area Coverage (GAC) record. The Global Area Coverage (GAC) data at 4 km nominal resolution from AVHRR from 1982 onwards provide one of the longest record of space based observations to date, spanning nearly 35 years. These multi-decadal data are extremely valuable for various climate applications ranging from studying large-scale processes, climate variability, to

	Doc:		Cloud_cci_D2.1_ATBD-RODC_v1.1.doc		
	Date:		28 August 2017		
	Issue:	1	Revision:	1	Page 5

assessing trends. However, when these missions were designed more than 40 years ago, the application of AVHRR data for climate purposes was not envisaged, at least not to the degree the scientific community realized it value few decades later. Therefore, for various planning, maintenance and economy reasons, NOAA satellites were allowed to drift from their stipulated sun-synchronous orbits during their life span (Ignatov et al. 2004). Figure 1-2 below shows the extent of this drifting for various satellites. Note that, the MetOps satellites that also carry AVHRR sensors were maintained in their orbit.

The direct impact of orbital drift of satellites is the gradual change in the time of observation. This creates many challenges, for example but not limited to, deducing physical trends from spurious ones. To make things complicated, Figure 1-2 shows that the rate of drift is different not only among satellites, but it can also change rapidly toward the end of lifespan of a particular satellite. This has implications for assessing the trends in the time-series' of geophysical variables retrieved from AVHRRs. Various studies have previously investigated the impact of orbital drift on geophysical variables such as outgoing longwave radiation, surface temperatures, vegetation indices, and clouds (Waliser and Zhou, 1997; Lucas et al. 2001; Jin and Treadon, 2003; Devasthale and Grassl, 2007; Devasthale et al. 2012; Foster and Heidinger, 2014; Nagol et al. 2014).

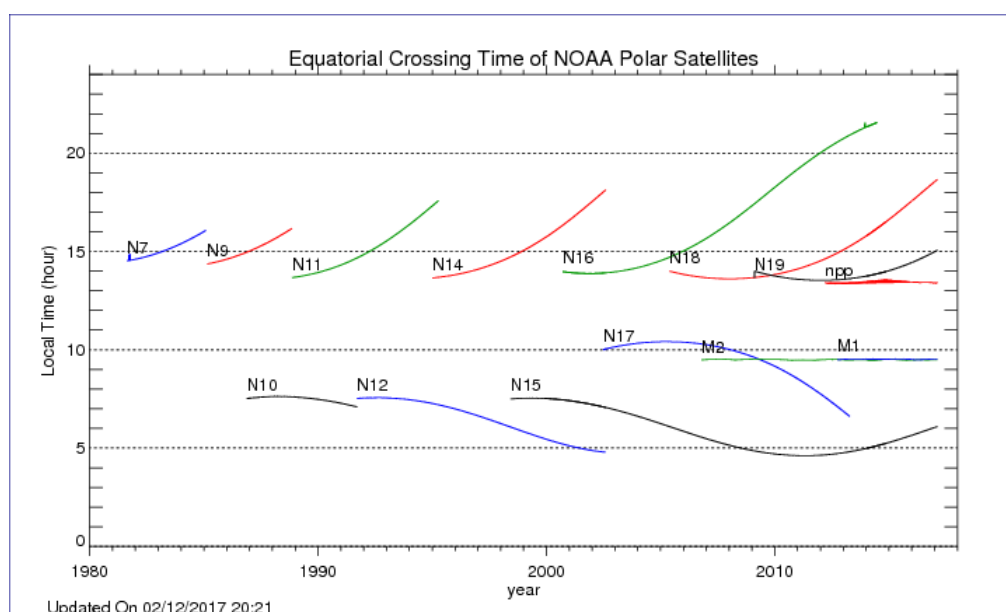



Figure 1-2 The equator crossing times of various NOAA and MetOp satellites

In the following section of this report the results of a Cloud_cci effort is presented which was dedicated to investigating potential impact of drifting on cloud properties and to suggest potential solution(s) that can be implemented in the later phases. Such assessment will help Cloud_cci data users to better understand the physicality of variability and trends deduced from the datasets.

	Doc:	Cloud_cci_D2.1_ATBD-RODC_v1.1.doc			
	Date:	28 August 2017			
	Issue:	1	Revision:	1	Page 6

2. Impact of orbital drift on clouds

There are two principle ways orbital drift can impact cloud retrievals from AVHRRs.

a) Inconsistent sampling of diurnal cycles

The constant change of observation leads to the fact that AVHRRs observe clouds during different stages of their life cycle. As illustrated schematically in Figure 2-1, it could lead to different effects, depending on whether clouds are being observed during their growth or during their decaying phase. It is well-known that the diurnal cycles of clouds depend on a number of factors, such as cloud type in question, season, geographical position, etc. The extent of the impact of clouds such as thin cirrus can be little due to relatively flatter diurnal cycle of these clouds, while the impact may be stronger for deep convective clouds that have diurnal cycle with large amplitudes. The diurnal cycle of stratocumulus regimes could be very flat in the higher latitudes in winter compared to summer months. This makes addressing the impact of orbital drift ever so complicated and difficult.

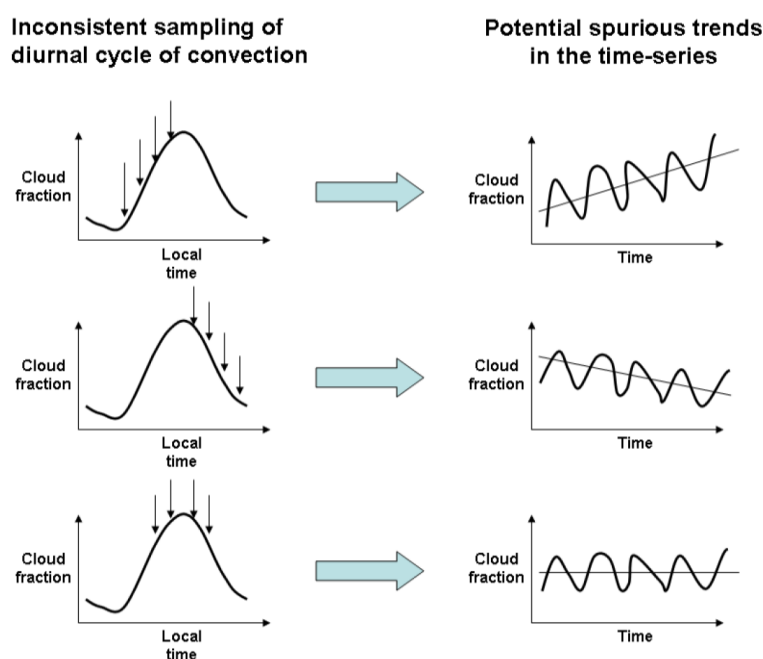



Figure 2-1 The conceptual diagram showing potential impact of orbital drift on the time series of cloud fraction (Figure taken from [Devasthale et al. 2012](#)).

b) Change in solar zenith angles

Change in observation time also implies change in the illumination conditions, i.e. solar zenith angles. Cloud property retrievals depend on zenith angles as various thresholds, offsets and look-up tables are either a function of or tuned using solar zenith angles. Therefore, the performance of a retrieval scheme is well-known to be sensitive to the illumination conditions, depending on how well this sensitivity is treated in the retrieval algorithm. Note that this effect is independent to inconsistent sampling of diurnal cycles, but they can work in conjunction to either dampen or worsen the overall impact of orbital drift on cloud property retrievals.

	Doc:		Cloud_cci_D2.1_ATBD-RODC_v1.1.doc		
	Date:		28 August 2017		
	Issue:	1	Revision:	1	Page 7

3. Possible approaches to account for orbital drift effect

There are two major schools of thoughts for identifying and correcting the orbital drift effect on cloud properties. These two approaches are discussed below. Each approach has its own advantage and disadvantage, which are also discussed.


a) Using rotated empirical orthogonal functions (REOFs)

Empirical orthogonal function is one of the techniques (similar to principal component analysis) to decompose information content to a number of basis functions with the advantage that both spatial and temporal patterns of EOFs can be useful to investigate artifacts caused by orbital drift. Furthermore, by rotating the EOFs (REOFs), the information can be reduced to a handful of modes. The main advantage of using REOFs lies in their ability to intrinsically delineate orbital drift signal (in both space and time) independent of any other information. The main disadvantages include domain dependence of the results and sometimes difficulty in interpreting physical features in the spatial patterns.

b) Using diurnal cycles to estimate correction

The second approach involves using diurnal cycles to correct the orbital drift signal. This approach relies heavily on the assumption that spatially and temporally resolved diurnal cycles of clouds are available on a global scale. Needless to say, this approach offers physically based corrections and involves less manual intervention compared to REOFs. But it is not always possible to disentangle orbital drift signal as vividly as in the case of REOFs and the reliance on the accuracy of diurnal cycles can be problematic.

Both of these approaches have their advantages and disadvantages and both of them were studied in the context of ESA Cloud_cci.

	Doc:		Cloud_cci_D2.1_ATBD-RODC_v1.1.doc		
	Date:		28 August 2017		
	Issue:	1	Revision:	1	Page 8

4. Application of diurnal cycle based methodology to ESA Cloud_cci AVHRR-AM/PM datasets


The following steps describe the methodology to correct orbital drift effect using an example of total cloud fraction for demonstration.

a) Computing diurnal cycles

The first step involves preparing climatological diurnal cycles at each grid point. Since both morning and afternoon satellites drifted in their orbits at different rates, it is possible to exploit this fact to compute climatological diurnal cycles. It is also important to use the same data to compute diurnal cycles for the sake of consistency and to avoid ambiguities arising from different retrieval schemes. All 33-yr Level 2b data from 1982 through 2014 were used to compute diurnal cycles at $1^{\circ} \times 1^{\circ}$ grid for each month and 3-hr time slot. The resulting climatological diurnal cycle data file has therefore four dimensions [180 x 360 x 12 x 8]. The Figure 4-1 and 4-2 below show examples of diurnally resolved climatological cloud fractions for January and July months respectively.

b) Fitting the sinusoidal curves to diurnal cycles

The climatological diurnal cycles could be “bumpy” in nature, in the sense that they may not follow a smooth rate of change with respect to time due to a number of reasons. For example, poor sampling at a particular time slot, uneven sensitivity of cloud masking scheme to the time of day, etc. Therefore, it is necessary to fit a sinusoidal curve to the observed diurnal cycle. Such fitting has both advantages and disadvantages as discussed later. But overall, the advantages are likely to outweigh the disadvantages, as proven later in the goodness-of-fit tests. Figure 4-3 below shows an example of curve fitting.

	Doc:	Cloud_cci_D2.1_ATBD-RODC_v1.1.doc		
	Date:	28 August 2017		
	Issue:	1	Revision:	1
Page 9				

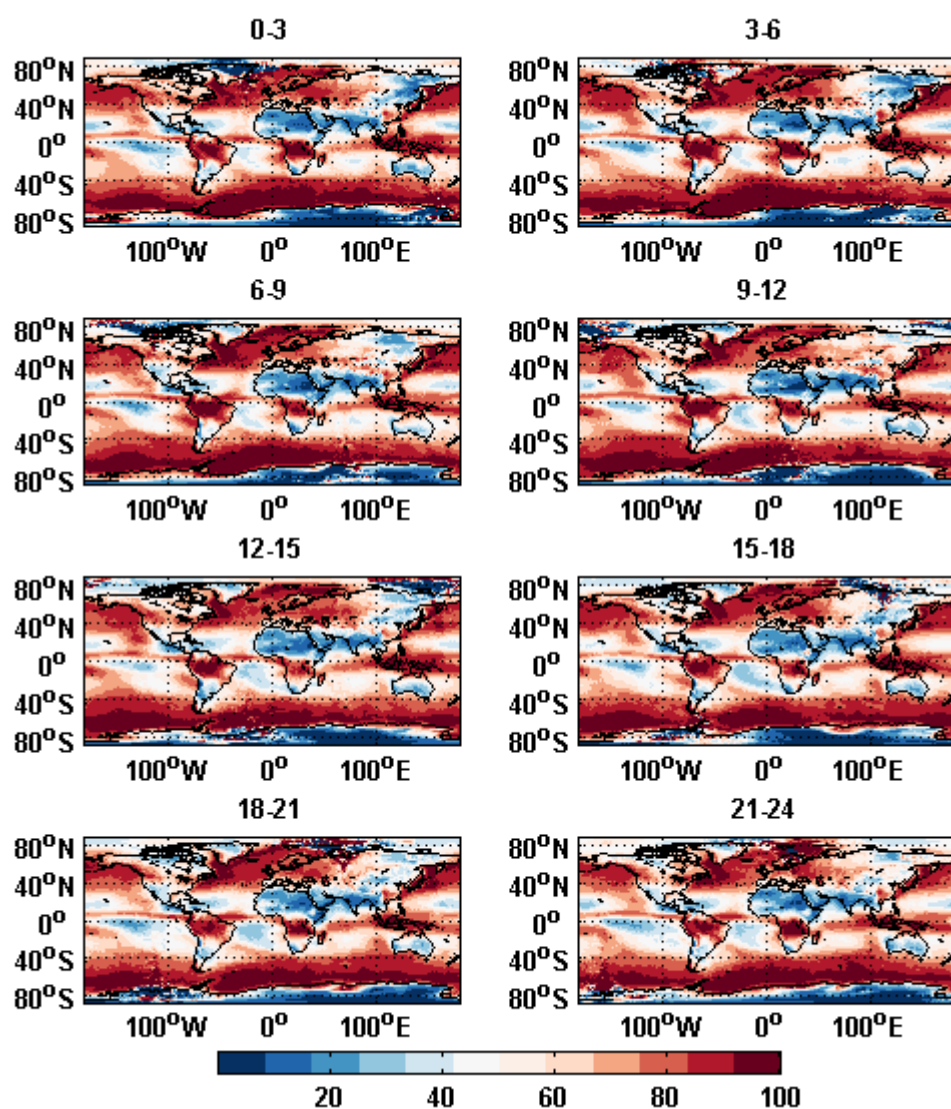



Figure 4-1 Climatological diurnal cycle of total cloud fraction for the month of January. The titles of the subplots indicate UTC times.

	Doc:	Cloud_cci_D2.1_ATBD-RODC_v1.1.doc		
	Date:	28 August 2017		
	Issue:	1	Revision:	1
Page 10				

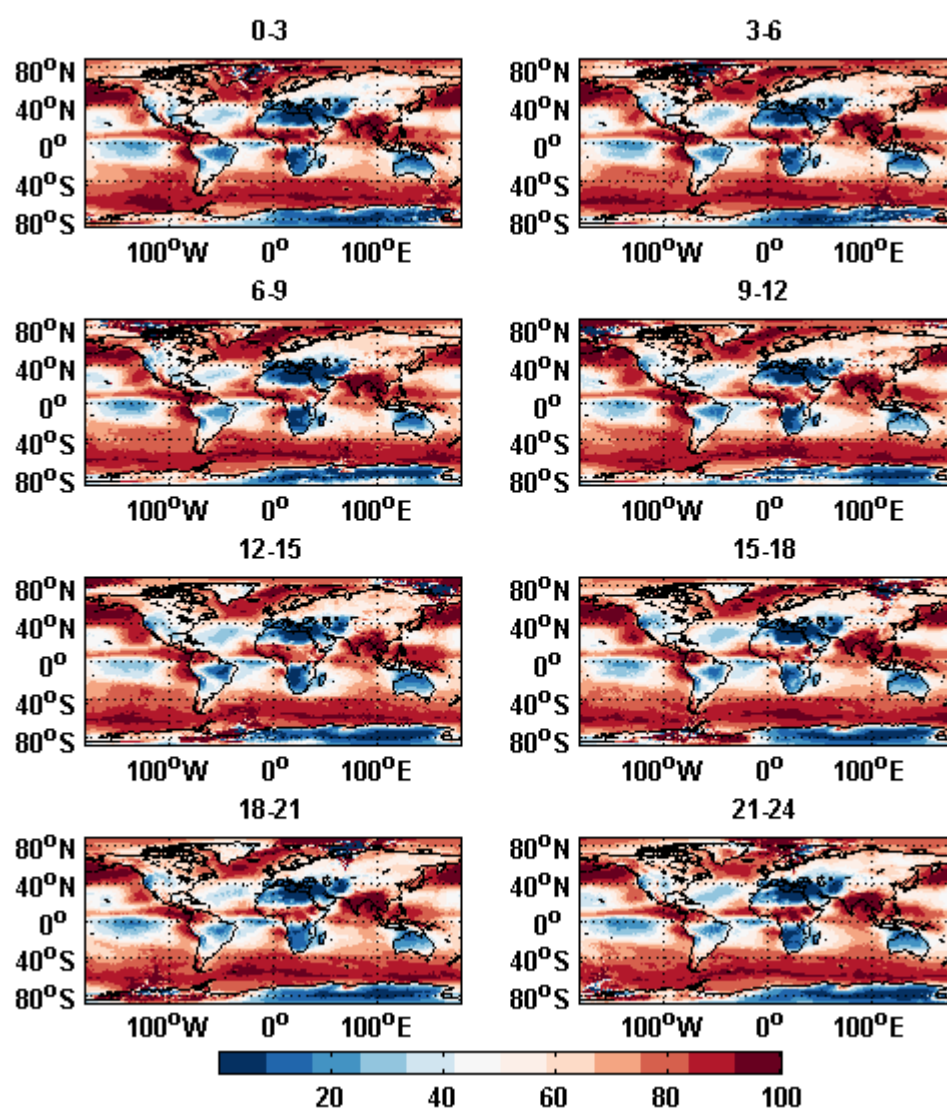


Figure 4-2 Climatological diurnal cycle of total cloud fraction for the month of July. The titles of the subplots indicate UTC times.

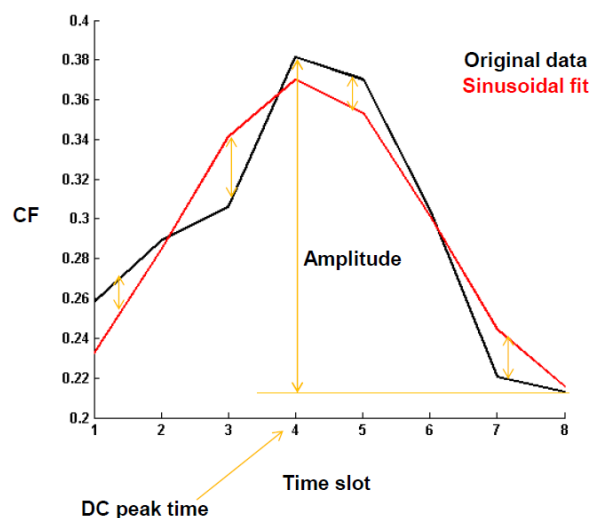


Figure 4-3 An arbitrary example of original and fitted diurnal cycle.

c) Fitting polynomial to equator crossing times

To apply corrections, the rate of drift needs to be calculated for each satellite. This is done by investigating the equator crossing times for each satellite and fitting a second degree polynomial as a function of days since launch as shown in Figure 4-4 below. These fitting coefficients are later used to estimate the magnitude of drift in time.

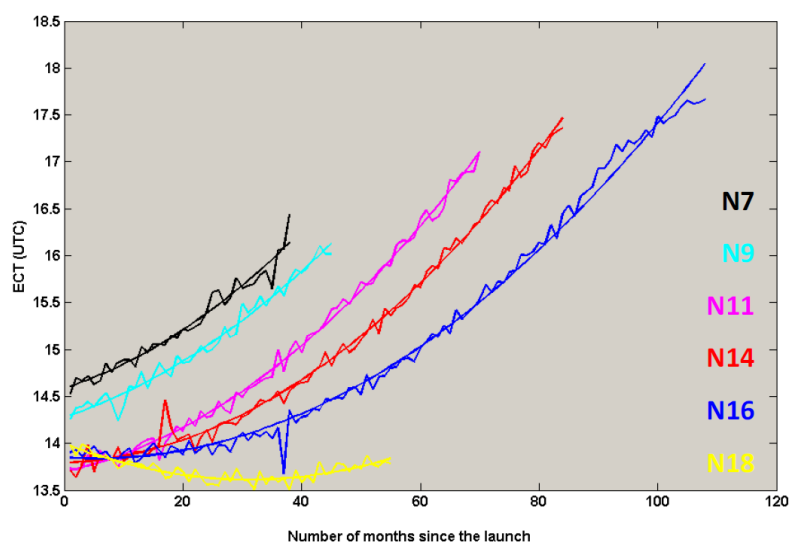



Figure 4-4 Fitting the second degree polynomial to the equator crossing times of various satellites.

	Doc:	Cloud_cci_D2.1_ATBD-RODC_v1.1.doc		
	Date:	28 August 2017		
	Issue:	1	Revision:	1
Page 12				

d) Retrieving the launch times

The global gridded maps of launch times are needed to estimate the starting cloud fraction expected from the diurnal cycles derived at each grid points. The Figure 4-5 below shows an example of such maps for various satellites. These maps are prepared for each satellite separately.

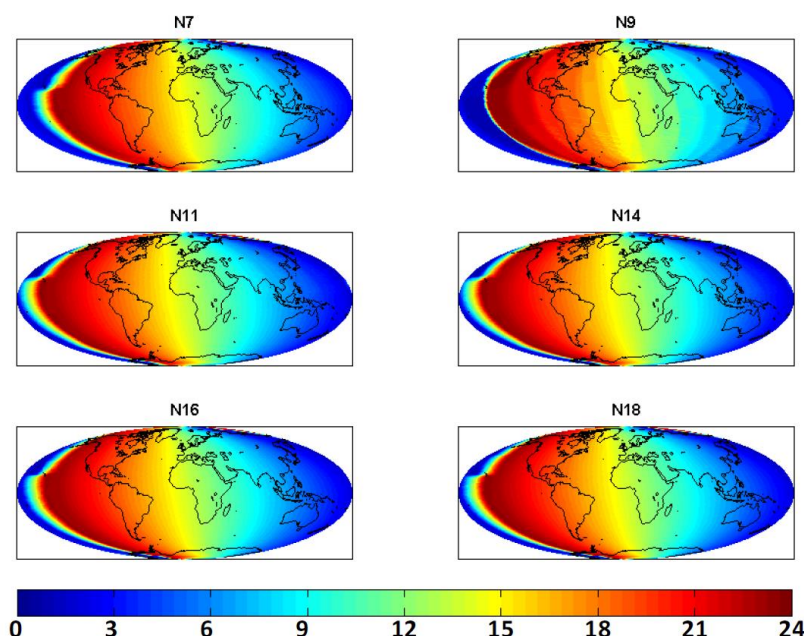



Figure 4-5 The UTC times at launch for various satellites.

e) Computing and applying the correction

The corrections are computed as follows. For each grid point, the rate of drift is estimated based on the polynomials mentioned above, considering difference between the UTC time at present and UTC time at launch. This information is mapped on the climatological diurnal cycles to estimate the percentage change in cloud fraction due to drifting between two points of time in question. The resulting delta change could be positive or negative depending on which segment of the diurnal cycle is required to be considered.

This delta amount is then added to the uncorrected cloud fraction, which will result in slight increase or decrease in original cloud fraction. Figure 4-6 below shows a time corrected and uncorrected monthly mean time series of total cloud fraction in the tropics (30N-30S), together with the difference. It can be clearly seen that the orbital drift signal is visible in the difference time series. However, the magnitude is small, mainly due to compensating effects from different regions. To highlight this fact, Figure 4-7 shows the spatial pattern of applied corrections for July 1994 for NOAA-11. These corrections are mainly negative over the majority of the convectively active regions in the ITCZ, indicating that the cloudiness was overestimated as a result of drift towards the end of NOAA-11 life span. The magnitude of corrections ranges from -10% to 18%, which is very significant. There is also strong spatial heterogeneity in the sign and magnitude of corrections.

	Doc:		Cloud_cci_D2.1_ATBD-RODC_v1.1.doc		
	Date:		28 August 2017		
	Issue:	1	Revision:	1	Page 13

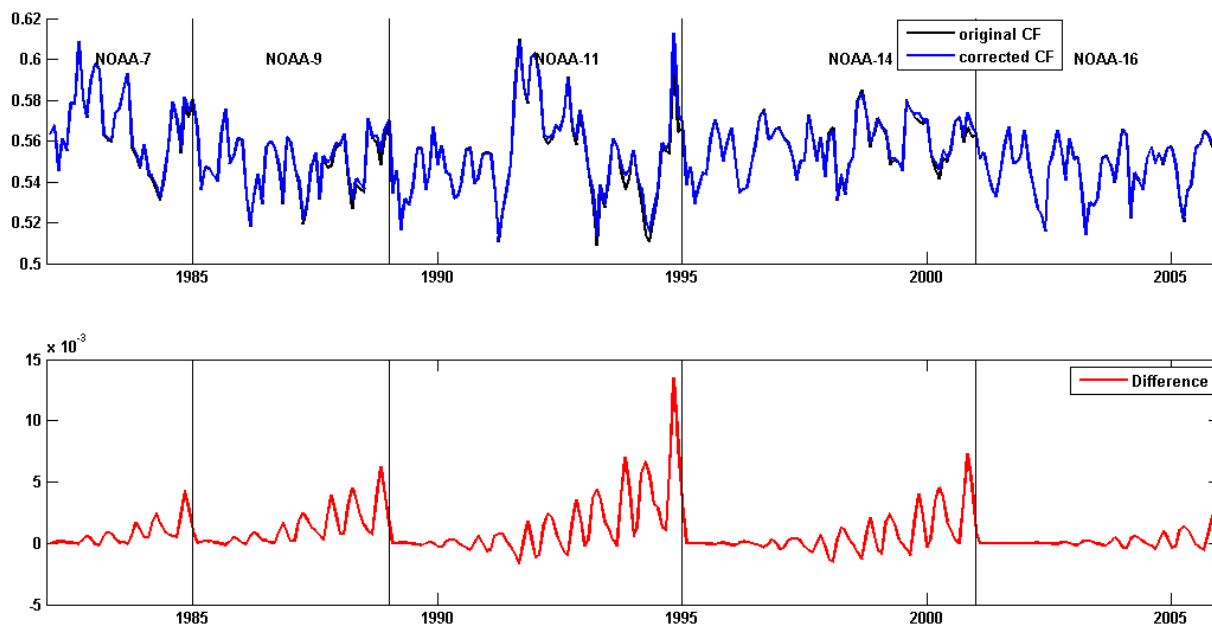


Figure 4-6 Corrected and uncorrected time series' of total cloud fraction in the tropics (30N-30S).

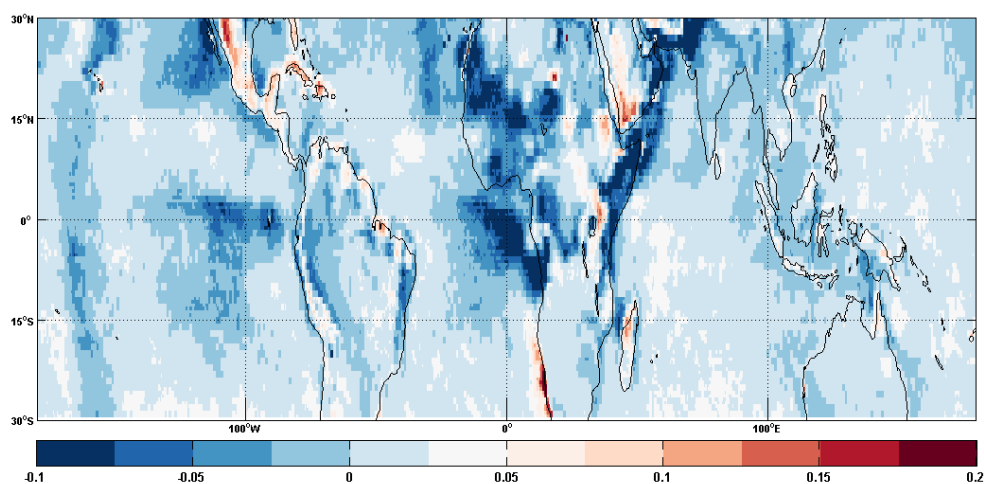


Figure 4-7 The spatial pattern of applied corrections for July 1994 for NOAA-11.

5. Evaluating diurnal cycles and some problem areas

a) Unsmooth diurnal cycles

Since this approach of orbital drift corrections is solely based on climatological diurnal cycles, it is important to critically evaluate how good diurnal cycles are resolved, their goodness of fit with sinusoids etc. Figure 5-1 below shows a few random examples of diurnal cycles and their sinusoidal fits based on ESA Cloud_cci and CM SAFs CLARA-A2 data (shown for comparison) (Schulz et al. 2009; Karlsson et al., 2009; 2016). A number of issues can be pointed out. In the first subplot, it is seen that during first half of the day, both CLARA-A2 and Cloud_cci diurnal cycles follow one another closely. However, during the latter part of the day, they start to drift, producing the difference of up to 10% in total cloud fraction. This has serious implication for drift corrections. If the uncorrected cloud fraction is observed during first half of the day, the magnitude of correction will be nearly similar in both datasets. But if uncorrected cloud fraction is observed during the latter part of the day, the correction could be under- or overestimated. The second subplot shows that the fitting preserves the respective times of peaks in CF and smoothens out the unphysical diurnal variations in the CF. The third subplot shows that the diurnal cycles in both datasets are quite flat. However, in the case of CLARA-A2 data, the cloud fraction in the final time slot suddenly jumps up forcing the corresponding sinusoidal fit to change its shape. The fourth subplot shows that while the peaks in uncorrected diurnal cycles are observed at different time, the fitting forces them to have diurnal variations.

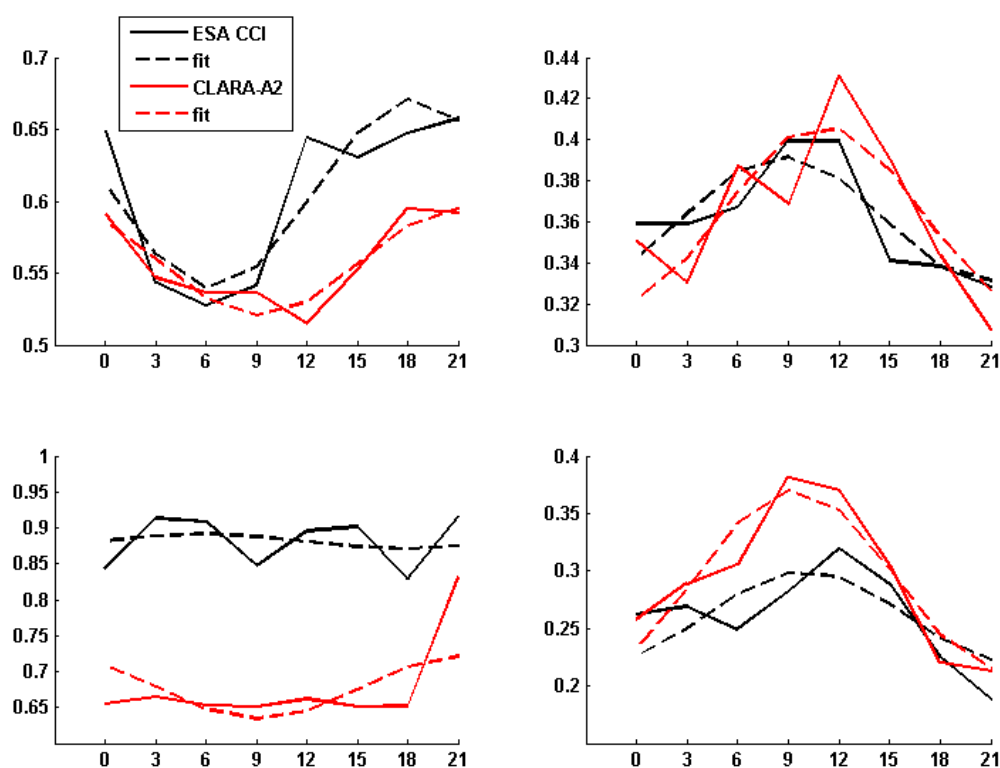



Figure 5-1 A few random examples of diurnal cycles of total cloud fraction and their sinusoidal fits based on ESA Cloud_cci and CLARA-A2 data.

	Doc:	Cloud_cci_D2.1_ATBD-RODC_v1.1.doc			
	Date:	28 August 2017			
	Issue:	1	Revision:	1	Page 15

b) How well do sinusoids agree with original diurnal cycles?

To address this question, in depth evaluations of goodness-of-fit are carried out using two metrics, root mean squared errors between sinusoids and original climatological diurnal cycles and the amplitude difference between them. Figure 5-2 below shows an example for the months of January and July. For comparison, the corresponding results from CLARA-A2 are also shown. In general, the RMSE values are below 5% and the amplitude differences are also less than 5%, indicating that the sinusoids are closely fitting to the original data. There are however problem areas/regions. For example, the polar regions, high latitude snow covered land regions etc. But in the majority of cases, climatological diurnal cycles can be approximated by sinusoids.

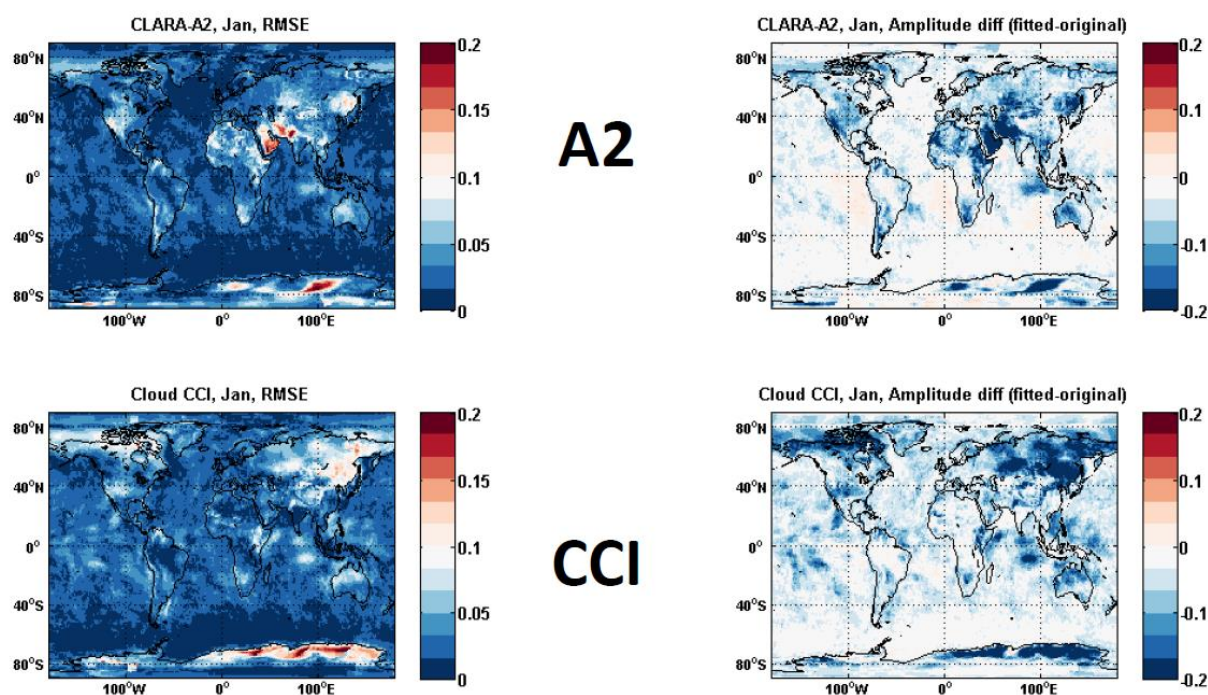



Figure 5-2 Evaluation of goodness-of-fit using two metrics, namely RMSE and amplitude difference. Data is for January and Cloud_cci (bottom row) and CLARA-A2 (top row) datasets.

	Doc:		Cloud_cci_D2.1_ATBD-RODC_v1.1.doc		
	Date:		28 August 2017		
	Issue:	1	Revision:	1	Page 16

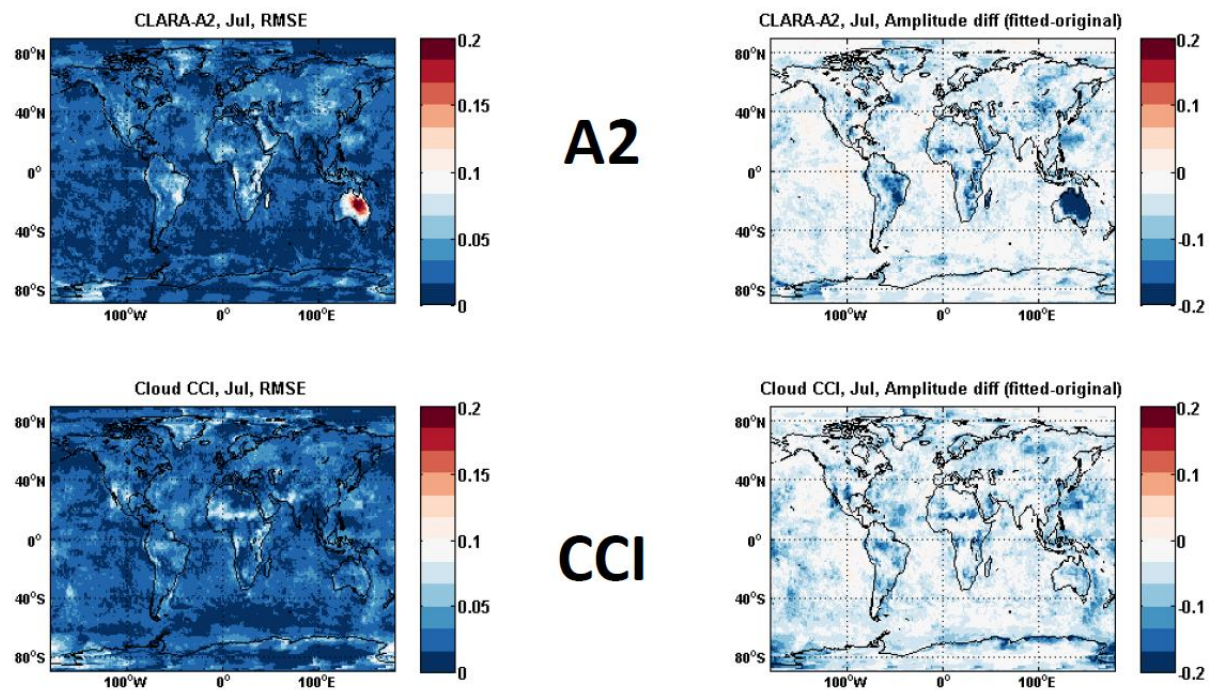



Figure 5-3 As Figure 5-2 but for July.

	Doc:	Cloud_cci_D2.1_ATBD-RODC_v1.1.doc		
	Date:	28 August 2017		
	Issue:	1	Revision:	1
Page 17				

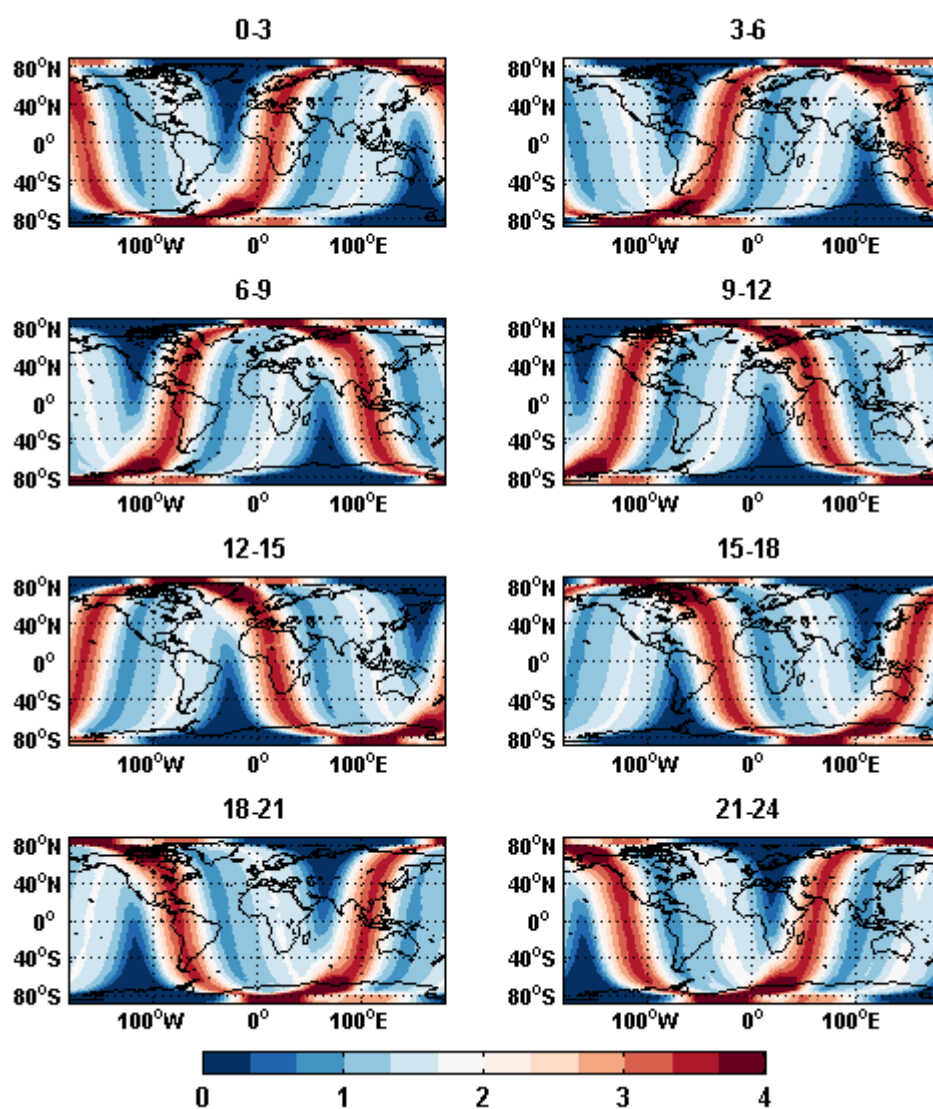



Figure 5-4 Total number of observations (x10⁵) available at each grid point and UTC time slot during 33-year period (1982-2014) for the month of July.

	Doc:	Cloud_cci_D2.1_ATBD-RODC_v1.1.doc			
	Date:	28 August 2017			
	Issue:	1	Revision:	1	Page 18

6. Applying REOFs to correct orbital drift effect

Before ESA Cloud_cci data were available, CM SAF's CLARA-A1 ([Karlsson et al., 2013](#)) data were used to prototype and investigate REOF methodology to correct orbital drift. The following sections summarize the work done in this context. It is to be noted that this exercise will be revised using the ESA Cloud_cci final dataset.

Step by step methodology

The practical methodology to correct for orbital drift signal is conceptually based on the original work of [Waliser and Zhou \(1997\)](#), [Lucas et al. \(2001\)](#) and [Devasthale et al \(2013\)](#). The corrected dataset can be obtained in six well-defined steps described below. A demonstration using an example of total daytime cloud fraction in the tropics based on 20 years of monthly mean CLARA-A1 data is provided where appropriate.

- First, the time series' (at each $1^\circ \times 1^\circ$ grid point) of monthly mean cloud fraction anomalies are prepared by subtracting the time series means.
- In the next step, an EOF analysis is performed and those modes are retained that explain the majority of variance (in this case 99%). Figure 6-1 below shows the spatial pattern of first four modes.

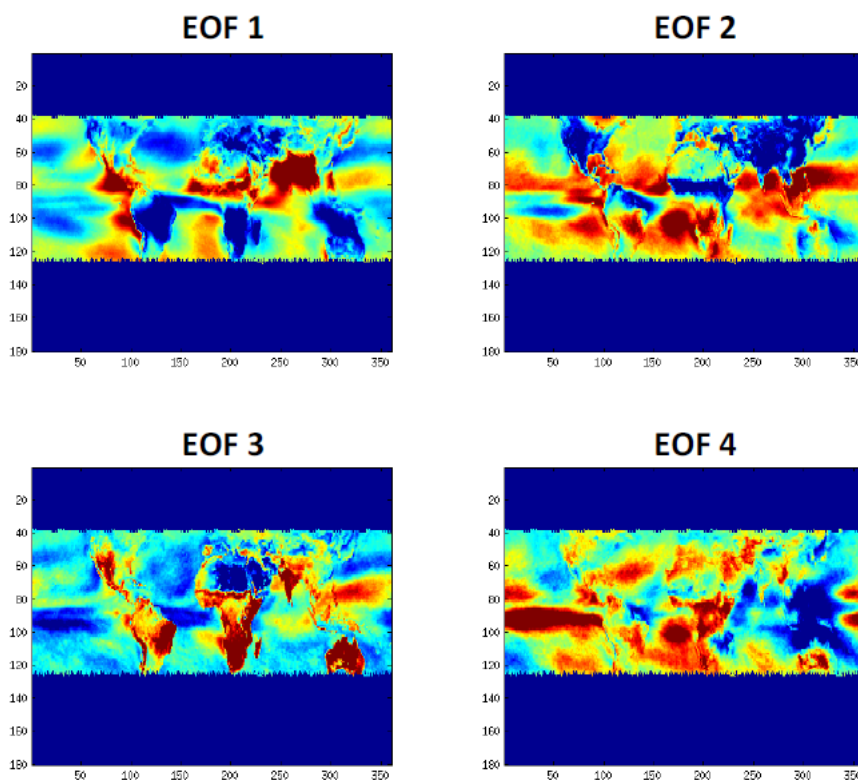


Figure 6-1 *The spatial pattern of first four modes of EOFs.*

- The EOF loadings, defined as the time series of the first chosen principal components (or EOF modes) are inspected visually and the modes that contain an orbital drift signal, i.e. resembling the increasing/decreasing trend during the life span of the sensor and then showing sudden jumps at the change of satellite and showing high correlation with equator crossing times, are identified.

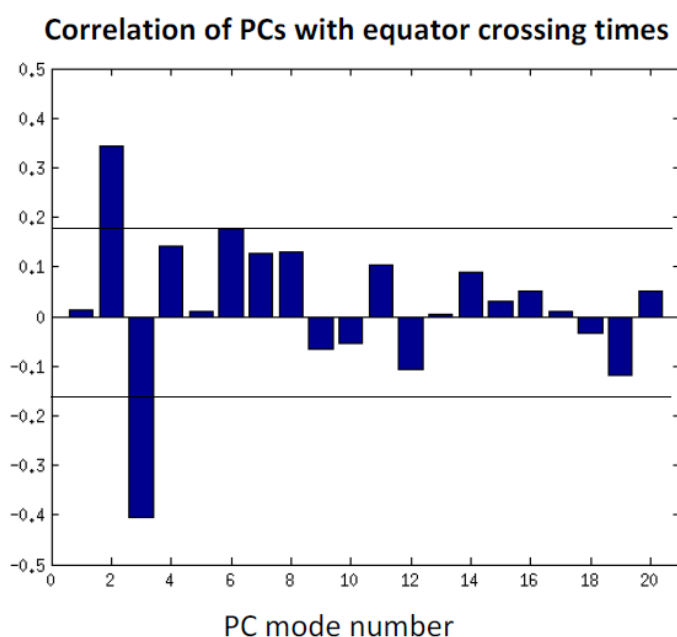


Figure 6-2 Correlation of first twenty principal components with equator crossing time. The mode numbers 2 and 3 show high correlation indicating possible contamination by orbital drift signal.

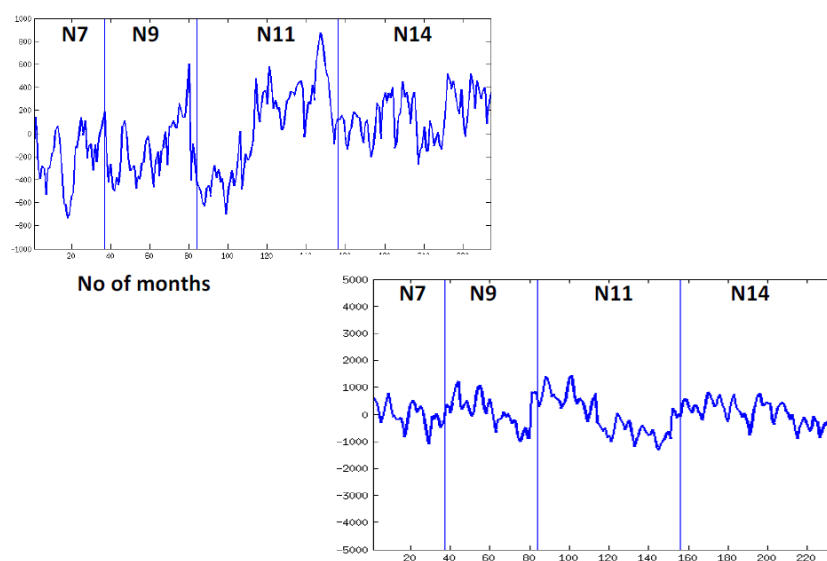



Figure 6-3 The time series of PC numbers 2 and 3 (mentioned in Figure 6-2 above) showing clear discontinuities in cloud fraction when the satellite platform is changed.

	Doc:	Cloud_cci_D2.1_ATBD-RODC_v1.1.doc			
	Date:	28 August 2017			
	Issue:	1	Revision:	1	Page 20

- The EOF loadings are rotated using the VARIMAX rotation (Kaiser, 1958; Richman, 1986). The correlation of PCs with equator crossing times was once again used to determine the number of nodes to be rotated.
- Synthetic loadings were then computed for these contaminated modes by fitting a linear regression between the EOF loadings and the local time of observation.
- These synthetic loadings were removed from the anomaly dataset. This yields a new dataset with the orbital drift signal removed.

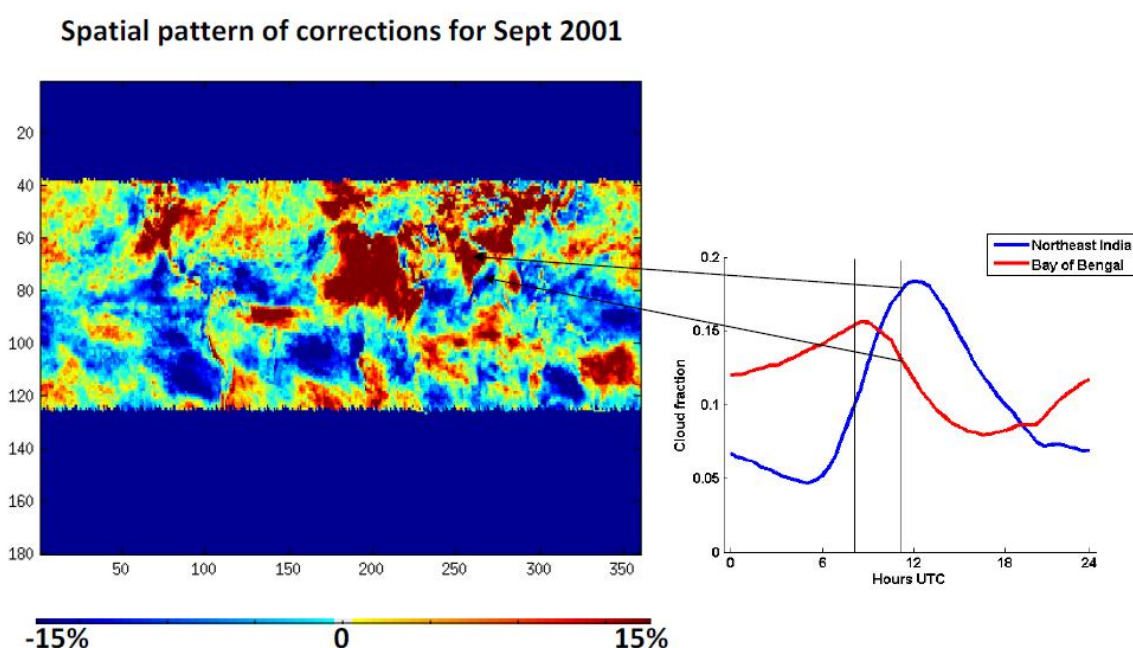




Figure 6-4 An example of the spatial pattern of corrections that need to be subtracted from the original NOAA-14 data for the month of Sept 2001. The positive corrections indicate the overestimation of cloud fraction. The diurnal cycles of cloudiness over continental India and Bay of Bengal explain why the corrections have different signs over those regions.

	Doc:		Cloud_cci_D2.1_ATBD-RODC_v1.1.doc		
	Date:		28 August 2017		
	Issue:	1	Revision:	1	Page 21

7. Summary

The main purpose of this task was to carry out a detailed feasibility study to determine how the orbital drift signal can be accounted for in the ESA Cloud_cci dataset. Two major approaches were considered and investigated for this purpose; one using empirical orthogonal functions and the other using diurnal cycles. While both of these approaches are suitable, each one has its own disadvantage. Considering the fact that the major improvements are seen in cloud masking procedures in recent years (a key requirement for obtaining accurate diurnal cycles) and the lessons learned during investigations of both approaches, the methodology employing diurnal cycles can be pursued further as it is more physically anchored. A manuscript is under preparation summarizing the applicability and strengths and weakness of both approaches to identify and correct orbital drift effect.

We propose following recommendations for the future work. Since the fidelity of orbital drift correction methodology depends on having accurate diurnal cycles, it is necessary that the climatological diurnal cycles of cloudiness are evaluated against an independent reference. For example, cloudiness data sets derived from high temporal resolution SEVIRI/MSG could be used over Europe and Africa for such evaluation. The goodness of fit of climatological diurnal cycles shall also be tested in such approach. Since the SEVIRI data record now spans more than 10+ years, it could also be used to check if the bias corrected cloudiness records from AVHRR are physical after applying orbital drift corrections over longer time periods (for example, in the cases of N-15 to N-18). An EOF analysis can be performed on the drift corrected datasets to cross check if any apparent artifacts are visible. The potential decadal climate change signal in clouds could very small. Therefore drift corrected data have to be evaluated in various ways to ensure that potential user is not misinterpreting artifacts with climate signals. While the focus of the present investigations has been exclusively on cloud fraction, similar recommendations also apply for other macro- and microphysical cloud properties.

	Doc:		Cloud_cci_D2.1_ATBD-RODC_v1.1.doc		
	Date:		28 August 2017		
	Issue:	1	Revision:	1	Page 22

8. References

Carbajal Henken, C.K., Lindstrot, R., Preusker, R. and Fischer, J., 2014: FAME-C: cloud property retrieval using synergistic AATSR and MERIS observations. *Atmos. Meas. Tech.*, 7, 3873-3890, doi:10.5194/amt-7-3873-2014.

Devasthale A., and H. Grassl, 2007: Dependence of frequency of convective cloud occurrence on the orbital drift of satellites, *Int. J. Remote Sens.*, 28, doi:10.1080/01431160701294646.

Devasthale, A., Karlsson, K.-G., Quaas, J., and Grassl, H., 2012: Correcting orbital drift signal in the time series of AVHRR derived convective cloud fraction using rotated empirical orthogonal function, *Atmos. Meas. Tech.*, 5, 267-273, doi:10.5194/amt-5-267-2012.

Foster, M.J.; Heidinger, A., 2013: PATMOS-x: Results from a diurnally corrected 30-yr satellite cloud climatology. *J. Clim.*, 26, 414-425.

Hannachi, A., T. Jolliffe, and D. B. Stephenson, 2007: Empirical orthogonal functions and related techniques in atmospheric science: A review, *Int. J. Clim.*, 27, 1119-1152.

Hollmann, R., Merchant, C.J., Saunders, R., Downy, C., Buchwitz, M., Cazenave, A., Chuvieco, E., Defourny, P., de Leeuw, G., Forsberg, R. and Holzer-Popp, T., 2013. The ESA climate change initiative: Satellite data records for essential climate variables. *Bulletin of the American Meteorological Society*, 94, 1541-1552.

Ignatov, A., I. Laszlo, E. D. Harrod, K. B. Kidwell, and G. P. Goodrum, 2004: Equator crossing times for NOAA, ERS and EOS sun-synchronous satellites, *Int. J. Remote Sens.*, 25, 5255-5266.

Jin, M. and R. E. Treadon, 2013: Correcting the orbit drift effect on AVHRR land surface skin temperature measurements, *Int. J. Remote Sens.*, 24, 4543-4558.

Kaiser, H. F., 1958: The varimax criterion for analytic rotation in factor analysis, *Psychometrika*, 23, 187-200.

Karlsson, K.-G., Riihelä, A., Müller, R., Meirink, J. F., Sedlar, J., Stengel, M., Lockhoff, M., Trentmann, J., Kaspar, F., Hollmann, R., and Wolters, E., 2013: CLARA-A1: a cloud, albedo, and radiation dataset from 28 yr of global AVHRR data, *Atmos. Chem. Phys.*, 13, 5351-5367, doi:10.5194/acp-13-5351-2013.

Karlsson, K.-G., Anttila, K., Trentmann, J., Stengel, M., Meirink, J. F., Devasthale, A., Hanschmann, T., Kothe, S., Jääskeläinen, E., Sedlar, J., Benas, N., van Zadelhoff, G.-J., Schlundt, C., Stein, D., Finkensieper, S., Håkansson, N., and Hollmann, R., 2017: CLARA-A2: The second edition of the CM SAF cloud and radiation data record from 34 years of global AVHRR data, *Atmos. Chem. Phys. Discuss.*, doi:10.5194/acp-2016-935, in review.


Lucas, L. E., D. E. Waliser, P. Xie, J. E. Janowiak, and B. Liebman, 2001: Estimating the satellite equatorial crossing time biases in the daily, global outgoing longwave radiation dataset, *J. Climate*, 14, 2583-2605.

McGarragh, G., Poulsen, C., Thomas, G., Povey, A., Sus, O., Schlundt, C., Stapelberg, S., Proud, S., Christensen, M., Stengel, M., and Grainger, R., 2017: The Community Cloud retrieval for CLimate (CC4CL). Part II: The optimal estimation algorithm, submitted to *Atmospheric Measurement Techniques Discussions*, pp.

Nagol, J.R.; Vermote, E.F.; Prince, S.D., 2014: Quantification of Impact of Orbital Drift on Inter-Annual Trends in AVHRR NDVI Data. *Remote Sens.*, 6, 6680-6687.

Richman, M. B., 1986: Rotation of principal components, *J. of Climatology*, 6, 293-335.


Schulz J., and co-authors, 2009: Operational climate monitoring from space: the EUMETSAT satellite application facility on climate monitoring (CM SAF), *Atmos. Chem. Phys.*, 9, 1687-1709.

	Doc:		Cloud_cci_D2.1_ATBD-RODC_v1.1.doc		
	Date:		28 August 2017		
	Issue:	1	Revision:	1	Page 23

Sus, O., Jerg, M., Poulsen, C., Thomas, G., Stapelberg, S., McGarragh, G., Povey, A., Schlundt, C., Stengel, M., and Hollmann, R., 2017: The Community Cloud retrieval for CLimate (CC4CL). Part I: A framework applied to multiple satellite imaging sensors, submitted to Atmospheric Measurement Techniques Discussions, pp. -.

Stengel, M., S. Mieruch, M. Jerg, K.-G. Karlsson, R. Scheirer, B. Maddux, J.F. Meirink, C. Poulsen, R. Siddans, A. Walther, and R. Hollmann, 2015: The Clouds Climate Change Initiative: Assessment of state-of-the-art cloud property retrieval schemes applied to AVHRR heritage measurements, Remote Sensing of Environment, <http://dx.doi.org/10.1016/j.rse.2013.10.035>

Waliser, D. E., and W. Zhou, 1997: Removing satellite equatorial crossing time biases from the OLR and HRC datasets, J. Climate, 10, 2125-2146.

	Doc:		Cloud_cci_D2.1_ATBD-RODC_v1.1.doc		
	Date:		28 August 2017		
	Issue:	1	Revision:	1	Page 24

9. Glossary

AATSR	Advanced Along Track Scanning Radiometer
AVHRR	Advanced Very High Resolution Radiometer
CC4CL	Community Cloud retrieval for Climate
ENVISAT	Environmental Satellite
ERS2	European Remote-sensing Satellite - 2
FAME-C	Freie Universität Berlin AATSR MERIS Cloud
MERIS	Medium Resolution Imaging Spectrometer
MODIS	Moderate Resolution Imaging Spectroradiometer
NOAA	National Oceanic and Atmospheric Administration